Chemical Science

ROYAL SOCIETY OF CHEMISTRY

EDGE ARTICLE

View Article Online
View Journal | View Issue

Open Access Article. Published on 13 May 2024. Downloaded on 8/2/2025 6:55:55 AM.
This article is licensed under a Creative Commons Attribution-NonCommercial 3.0 Unported Licence.

Check for updates

Cite this: *Chem. Sci.*, 2024, **15**, 8786

All publication charges for this article have been paid for by the Royal Society of Chemistry

# Convergence criteria for single-step free-energy calculations: the relation between the Π bias measure and the sample variance†

Meiting Wang,[ab] Ye Mei*[cde] and Ulf Ryde*[b]

Received 8th January 2024
Accepted 8th May 2024

DOI: 10.1039/d4sc00140k

rsc.li/chemical-science

Free energy calculations play a crucial role in simulating chemical processes, enzymatic reactions, and drug design. However, assessing the reliability and convergence of these calculations remains a challenge. This study focuses on single-step free-energy calculations using thermodynamic perturbation. It explores how the sample distributions influence the estimated results and evaluates the reliability of various convergence criteria, including Kofke's bias measure Π and the standard deviation of the energy difference $\Delta U$, $\sigma_{\Delta U}$. The findings reveal that for Gaussian distributions, there is a straightforward relationship between Π and $\sigma_{\Delta U}$, free energies can be accurately approximated using a second-order cumulant expansion, and reliable results are attainable for $\sigma_{\Delta U}$ up to 25 kcal mol$^{-1}$. However, interpreting non-Gaussian distributions is more complex. If the distribution is skewed towards more positive values than a Gaussian, converging the free energy becomes easier, rendering standard convergence criteria overly stringent. Conversely, distributions that are skewed towards more negative values than a Gaussian present greater challenges in achieving convergence, making standard criteria unreliable. We propose a practical approach to assess the convergence of estimated free energies.

## Introduction

Free energies play a pivotal role in determining the thermodynamic feasibility of processes. Therefore, there has been much interest in both measuring and calculating free energies. The most accurate technique to calculate the free-energy difference between two thermodynamic states involves performing a gradual transformation along a pathway connecting these states.[1–5] During this process, the energy difference is accumulated while conformations are sampled, typically through molecular dynamics or Monte Carlo simulations using molecular mechanics (MM) potential. However, the accuracy of MM calculations is known to be limited.[6–8] Consequently, many scientists are actively engaged in developing methods to calculate free energies using quantum mechanical (QM) methods, which promise enhanced accuracy and reliability.[9–15]

The reference-potential approach, also known as the dual-Hamiltonian approach, is an efficient method to calculate free-energy differences and profiles at either a QM or hybrid QM and molecular mechanics (QM/MM) level (hereafter collectively referred to as QM for simplicity). This approach, which avoids direct sampling at the QM level, was independently proposed by Gao and by Warshel in 1992.[16,17] Since its introduction, it has seen widespread applications and enhancements by various groups for predicting binding affinities, solvation free energies, and reaction barriers.[13,15,18–25] The method involves performing sampling at a lower theoretical level, such as MM, and then obtaining the free-energy difference at the QM level through a free-energy correction from the change of the energy function from MM to QM. As depicted in the thermodynamic cycle in Fig. 1, the free-energy difference between states A and B at the QM level can be calculated as $\Delta G^{\mathrm{QM}}_{\mathrm{A}\to\mathrm{B}} = \Delta G^{\mathrm{MM}}_{\mathrm{A}\to\mathrm{B}} - \Delta G^{\mathrm{MM}\to\mathrm{QM}}_{\mathrm{A}} + \Delta G^{\mathrm{MM}\to\mathrm{QM}}_{\mathrm{B}}$, exploiting the fact that the free energy is a state function.

The primary objective of reference-potential methods is to achieve high accuracy at an affordable computational cost. Simulations on a QM potential-energy surface are exceedingly time-intensive, often making the direct calculation of the free-energy difference $\Delta G^{\mathrm{QM}}_{\mathrm{A}\to\mathrm{B}}$ prohibitively expensive. In contrast, calculating $\Delta G^{\mathrm{MM}}_{\mathrm{A}\to\mathrm{B}}$ at the MM level is more feasible. Therefore, the free-energy differences $\Delta G^{\mathrm{MM}\to\mathrm{QM}}_{\mathrm{A}}$ and $\Delta G^{\mathrm{MM}\to\mathrm{QM}}_{\mathrm{B}}$ need to be obtained without QM simulations, achievable through

[a]School of Medical Engineering & Henan International Joint Laboratory of Neural Information Analysis and Drug Intelligent Design, Xinxiang Medical University, Xinxiang 453003, China

[b]Department of Computational Chemistry, Lund University, Chemical Centre, P.O. Box 124, SE-221 00 Lund, Sweden. E-mail: ulf.ryde@compchem.lu.se

[c]State Key Laboratory of Precision Spectroscopy, School of Physics and Electronic Science, East China Normal University, Shanghai 200241, China. E-mail: ymei@phy.ecnu.edu.cn

[d]NYU-ECNU Center for Computational Chemistry at NYU Shanghai, Shanghai 200062, China

[e]Collaborative Innovation Center of Extreme Optics, Shanxi University, Taiyuan, Shanxi 030006, China

† Electronic supplementary information (ESI) available. See DOI: https://doi.org/10.1039/d4sc00140k



© 2024 The Author(s). Published by the Royal Society of Chemistry

Open Access Article. Published on 13 May 2024. Downloaded on 8/2/2025 6:55:55 AM.
This article is licensed under a Creative Commons Attribution-NonCommercial 3.0 Unported Licence.

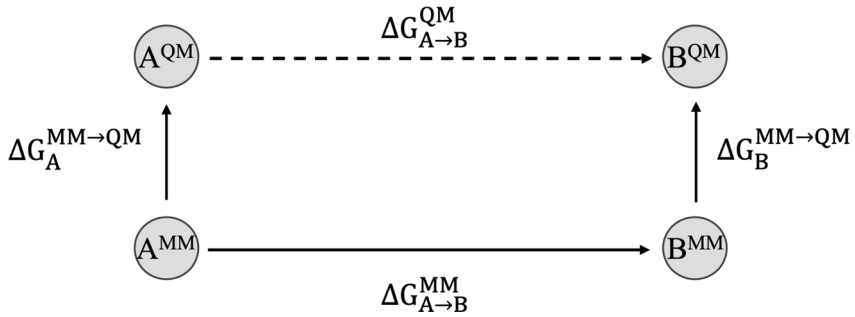


Fig. 1 The reference-potential approach.

single-step thermodynamic perturbations[26] (TP; also known as exponential averaging or free-energy perturbation). This is in stark contrast to other methods like thermodynamic integration (TI),[27] Bennett acceptance ratio (BAR)[28] or its multi-state variant (MBAR),[29] which require at least one simulation on the QM potential-energy surface, resulting in substantially higher computational demands.

Unfortunately, computing $\Delta G^{\mathrm{MM}\to\mathrm{QM}}$ is problematic. Numerous studies have highlighted that the convergence of free-energy differences calculated using TP is often slow and the reliability of the results is frequently questionable.[13,25,30–32] Therefore, it is essential to rigorously verify the convergence of the $\Delta G^{\mathrm{MM}\to\mathrm{QM}}$ calculations to ensure their trustworthiness before relying on the results. This is crucial to ensure the overall accuracy and reliability of the reference-potential methods.

Therefore, establishing reliable convergence measures for the calculated $\Delta G^{\mathrm{MM}\to\mathrm{QM}}$ is highly valuable. Numerous studies have explored various convergence criteria for TP calculations.[15,25,33–37] It has been noted that convergence is influenced by the variance of the energy difference between the two Hamiltonians, ${\sigma_{\Delta U}}^2$ ($\Delta U = U^{\mathrm{QM}} - U^{\mathrm{MM}}$). Some studies[38,39] have recommended that $\sigma_{\Delta U}$ should be kept below 1–2 $k_{\mathrm{B}}T$, where $k_{\mathrm{B}}$ is Boltzmann's constant and $T$ is the absolute temperature. This recommendation translates at 300 K to 0.6–1.2 kcal mol$^{-1}$, which is quite stringent. Later studies propose that 4 $k_{\mathrm{B}}T$ (equivalent to 2.3 kcal mol$^{-1}$) may be a more practical threshold.[34] Additionally, the weight of each configuration in the exponential average, $w_i = \frac{\mathrm{e}^{-\Delta U_i/k_{\mathrm{B}}T}}{\sum_{i=0}^{N}\mathrm{e}^{-\Delta U_i/k_{\mathrm{B}}T}}$ has also been considered for assessing convergence. If the average is dominated by one or only a few values, it may indicate unreliability.[40,41] Another proposed metric is the reweighting entropy,.[15] $S_w = -\frac{1}{\ln N}\sum_{i=0}^{N} w_i \ln w_i$. It has been suggested that an $S_w$ value less than 0.65 could signal that the predicted result might be unreliable.[15]

The bias measure Π, formulated by Kofke and co-workers,[42–47] serves as another tool for quantifying the convergence of TP calculations. It is advised that the value of Π should exceed 0.5 for converged calculations.[13,34,43,44] However, it is important to note that the Π bias measure is based on certain assumptions, such as the energy difference $\Delta U$ follows a Gaussian distribution. Consequently, this criterion might not be universally applicable in all scenarios, especially in cases where $\Delta U$ deviates from a Gaussian distribution. This highlights the importance of understanding the underlying assumptions and limitations of convergence measures in TP calculations.

Identifying a unique comprehensive convergence criterion for TP is nontrivial. In the current study, we establish the relationship between the bias metrics Π and $\sigma_{\Delta U}$. Subsequently, we employ various statistical probability distributions to examine the influence of both distribution and $\sigma_{\Delta U}$ on the convergence of TP calculations. Ultimately, this leads us to propose a practical approach for assessing the accuracy of computed free energy values.

## Theory and methods

### Free-energy estimators

As mentioned in the introduction, TP is the only practically feasible method to obtain $\Delta G^{\mathrm{MM}\to\mathrm{QM}}$ in the reference-potential method if time-consuming QM simulations should be avoided. With TP, the free-energy difference is calculated by

$$\Delta G^{\mathrm{MM}\to\mathrm{QM}} = -k_{\mathrm{B}}T\ln\left\langle \exp\left(-\frac{\Delta U}{k_{\mathrm{B}}T}\right)\right\rangle_{\mathrm{MM}}, \tag{1}$$

where $\langle\cdot\rangle_{\mathrm{MM}}$ denotes an average over the conformations sampled on the MM potential energy surface.

Such an exponential average suffers from a slow convergence with a finite number of samples.[36,37,48] In particular, the average may be dominated by a small number of terms with the most negative $\Delta U$ values. Therefore, many studies have suggested avoiding the use of Zwanzig's equation directly.[30,36,49,50] An alternative is to employ the cumulant approximation (CA):

$$\begin{aligned}\Delta G &= \sum_{k=1}^{\infty}\frac{-1^{k-1}}{(k_{\mathrm{B}}T)^{k-1}k!}C_{\mathrm{k}}\\ &= \langle\Delta U\rangle - \frac{{\sigma_{\Delta U}}^2}{2k_{\mathrm{B}}T} + \sum_{k=3}^{\infty}\frac{-1^{k-1}}{(k_{\mathrm{B}}T)^{k-1}k!}C_{\mathrm{k}}.\end{aligned} \tag{2}$$

Here, $C_k$ is the $k$th cumulant, of which the first two terms are the sample mean, $\langle\Delta U\rangle$, and the variance, ${\sigma_{\Delta U}}^2$, of the energy differences $\Delta U$, as indicated in the second line of eqn (2). If $\Delta U$

Open Access Article. Published on 13 May 2024. Downloaded on 8/2/2025 6:55:55 AM.
This article is licensed under a Creative Commons Attribution-NonCommercial 3.0 Unported Licence.

follows a Gaussian distribution, the cumulants of the third and higher order terms vanish, and thus eqn (2) can be written as

$$\Delta G = \langle \Delta U \rangle - \frac{{\sigma_{\Delta U}}^2}{2k_{\mathrm{B}}T}. \tag{3}$$

The CA truncated after the second-order term usually shows much better convergence properties than the exponential average in eqn (1). However, if $\Delta U$ deviates from a Gaussian distribution, the convergence and accuracy of the truncated CA are unclear.

### The bias measure Π

For a real simulation, the free-energy difference is estimated from finite samples. The distribution of $\Delta U$ may not be Gaussian and the phase-space overlap may not be sufficient. To check the reliability of the free-energy calculation, reliable convergence criteria are needed. Based on an idea from information theory, Wu and Kofke[43,44] suggested the Π bias measure, which is calculated from:

$$\Pi = \sqrt{W_{\mathrm{L}}\left[\frac{(N-1)^2}{2\pi}\right]} - \sqrt{\frac{2(\langle \Delta U \rangle - \Delta G)}{k_{\mathrm{B}}T}} \tag{4}$$

Here, $W_{\mathrm{L}}$ is the Lambert function, and $N$ is the sample size. It should be emphasized that the derivation of eqn (4) was based on two conditions: *viz.* that the distributions of forward and backward directions (*i.e.* in our case MM → QM and QM → MM) have identical variances and that $\Delta U$ follows a Gaussian distribution.

### Analytical model data

In general, the underlying distribution of $\Delta U$ is unknown, and therefore also the convergence properties of $\Delta G$. We have evaluated the convergence of $\Delta G$ by numerical simulations using several assumed statistical distributions, testing different shapes of the distributions. We typically test three different values of $\sigma_{\Delta U}$, 0.5, 1.0 and 2.0 kcal mol$^{-1}$, representing values below, within and outside the previously suggested convergence limit of 1–2 $k_{\mathrm{B}}T$ (0.6–1.2 kcal mol$^{-1}$). We used five distributions, which are described by the probability density function, $\rho(\Delta U)$ below. However, we first note that in terms of $\rho(\Delta U)$, eqn (1) can be rewritten as:

$$\Delta G = -k_{\mathrm{B}}T \ln \int_{-\infty}^{+\infty} \mathrm{e}^{-\frac{\Delta U}{k_{\mathrm{B}}T}} \rho(\Delta U) \mathrm{d}(\Delta U) \tag{5}$$

First, we used Gaussian distributions with the probability density function:

$$\rho_{\mathrm{Gaus}}(x;\mu,\sigma) = \frac{1}{\sigma\sqrt{2\pi}} \mathrm{e}^{-\frac{(x-\mu)^2}{2\sigma^2}} \tag{6}$$

where $\mu$ and $\sigma$ are the mean and standard deviation respectively.

Second, we used two types of Gumbel distributions. They are asymmetric distributions but do not deviate very much from a Gaussian distribution. Compared to a Gaussian distribution, Gumb_r decays slower on the right (positive) side of the main peak but faster on the left (negative) side, whereas the opposite applies to the Gumb_l distribution, as is shown in Fig. 2. The probability density functions of these two distributions are:

$$\rho_{\mathrm{Gumb_r}}(x;\mu,\beta) = \frac{1}{\beta} \mathrm{e}^{-(x-\mu)/\beta - \mathrm{e}^{-(x-\mu)/\beta}}, \tag{7}$$

and

$$\rho_{\mathrm{Gumb_l}}(x;\mu,\beta) = \frac{1}{\beta} \mathrm{e}^{(x-\mu)/\beta - \mathrm{e}^{(x-\mu)/\beta}}, \tag{8}$$

respectively, where $\mu$ is a location parameter and $\beta$ is a scale parameter. We adapted $\beta$ so that the distributions have standard deviations of 0.5, 1, and 2.

Third, we used Student's *t*-distribution. It is similar to the Gaussian distribution, but it has slightly wider distributions on both sides (*cf.* Fig. 2):

$$\rho_{\mathrm{t}}(x,\nu) = \left(\frac{\nu}{\nu + x^2}\right)^{\left(\frac{1+\nu}{2}\right)}, \tag{9}$$

where $\nu$ is the degrees of freedom. In this work, we used $\nu = 10$, which gives a distribution with a standard deviation of 1.12.

Fourth, we used the Beta distribution, which is a versatile set of asymmetric distributions:

$$\rho_{\mathrm{Beta}}(\xi,a,b) = \xi^{a-1}(1-\xi)^{b-1}\frac{\Gamma(a+b)}{\Gamma(a)\Gamma(b)} \tag{10}$$

where $\Gamma(z)$ is the gamma function. It is defined over the range $0 < \xi < 1$ (we used $\xi = x/5$, so $0 < x < 5$). We selected $a = 15$ and $b = 4$, which give $\sigma = 0.46$ and a single peak but with more positive outliers compared to a Gaussian distribution.

All model distributions used in this work are summarized in Table 1 and they are shown in Fig. 2.

We employed simple Python programs to simulate these distributions of the energy differences $\Delta U$. Numpy was employed to generate random numbers that follow these distributions. Autocorrelation functions were used to ensure that the random numbers were uncorrelated (*cf.* Fig. S1†). Moreover, the QUADPACK numerical quadrature routines were used to integrate eqn (5). The free-energy differences were calculated with both the exponential average and the second-order cumulant expansion (eqn (1) and (3)). Finally, the corresponding Π bias measure was calculated according to eqn (4). The Python codes employed are available upon request. Of course, all model distributions are unitless. The kcal mol$^{-1}$ energy units are introduced by the $k_{\mathrm{B}}T$ term, *e.g.* in eqn (5).

It should be pointed out that for the Gaussian, Gumb_r and Beta distributions, eqn (5) can be integrated numerically. However, the integration diverges for Gumb_l and Student *t*-10 distributions. In this work, the integration limits for Gumb0_l and Gumb1_l were set to −15 and 15, whereas for the Stud. *t*-10 and Gumb2_l distributions, the limits were [−20 20] and [−30 30], respectively. The probability for numbers outside these ranges is extremely small. This is confirmed by our random-number simulations, using sample sizes from 100 to 10

 © 2024 The Author(s). Published by the Royal Society of Chemistry

Open Access Article. Published on 13 May 2024. Downloaded on 8/2/2025 6:55:55 AM.
This article is licensed under a Creative Commons Attribution-NonCommercial 3.0 Unported Licence.

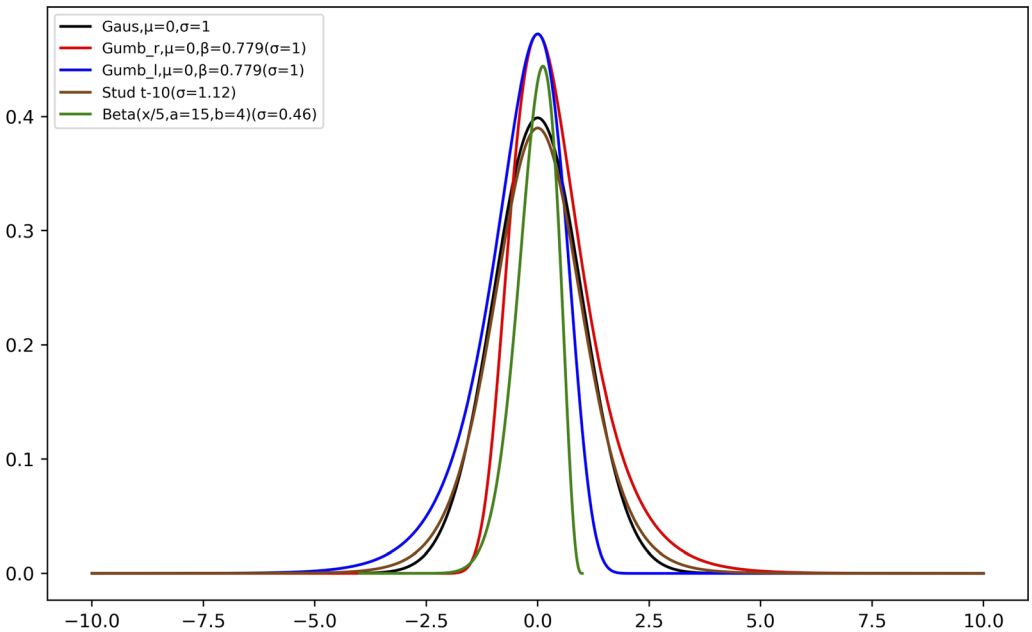


Fig. 2 The probability density of the model distributions employed. The probability of the Beta distribution was scaled (dividing the original value by 10) and the distribution has been translocated to overlap with the other distributions.

Table 1 Overview of the employed model distributions

| Abbreviation | Distribution | $\sigma$ |
|---|---|---|
| Gaus0 | Gaussian, $\mu = 0$ | 0.50 |
| Gaus1 | Gaussian, $\mu = 0$ | 1.00 |
| Gaus2 | Gaussian, $\mu = 0$ | 2.00 |
| Gaus3 | Gaussian, $\mu = 0$ | 3.00 |
| Gumb0_r | Gumbel_r, $\mu = 0$, $\beta = 0.39$ | 0.50 |
| Gumb1_r | Gumbel_r, $\mu = 0$, $\beta = 0.78$ | 1.00 |
| Gumb2_r | Gumbel_r, $\mu = 0$, $\beta = 1.56$ | 2.00 |
| Gumb0_l | Gumbel_l, $\mu = 0$, $\beta = 0.39$ | 0.50 |
| Gumb1_l | Gumbel_l, $\mu = 0$, $\beta = 0.78$ | 1.00 |
| Gumb2_l | Gumbel_l, $\mu = 0$, $\beta = 1.56$ | 2.00 |
| Stud. *t*-10 | Student's $t$, $\nu = 10$ | 1.12 |
| Beta | Beta, $\xi = x/5$, $a = 15$, $b = 4$ | 0.46 |

million data points. Thus, we have employed truncated distributions in the same way as in previous studies.[34]

## Results and discussion

### Effect of distribution

To investigate the impact of sample distributions on the calculated results, $\Delta G$ was estimated with both thermodynamic perturbation (TP; eqn (1)) and the second-order cumulant expansion (CA; eqn (3)). The result of the numerical integration of eqn (5) (NI) was taken as the reference. $\Delta G$ was calculated using 10 million data points for each distribution and the calculation was repeated 1000 times to estimate the standard deviation of the calculated values. The results are collected in Table 2.

Many studies have reported that the convergence of TP is strongly correlated to the variance ($\sigma_{\Delta U}{}^2$), and it has been suggested that converged results are obtained only if $\sigma_{\Delta U} < 0.6$–1.2 kcal mol$^{-1}$.[15,25,33–39] The results in Table 2 show that for Gaussian distributions with $\sigma_{\Delta U} = 0.5$ and 1.0 kcal mol$^{-1}$, both the TP and CA methods give excellent estimated free energies that coincide with that obtained with numerical integration. The $\Pi$ bias measure is also good, 3.5–4.4. However, when $\sigma_{\Delta U}$ is increased for the Gaussian distributions, the TP results start to deteriorate. For $\sigma_{\Delta U} = 2$ kcal mol$^{-1}$, the error for TP is only 0.01 kcal mol$^{-1}$, and the corresponding standard deviation and $\Pi$ value are 0.03 kcal mol$^{-1}$ and 1.9, respectively, indicating a satisfying convergence (with 10 million samples). However, for $\sigma_{\Delta U} = 3$ kcal mol$^{-1}$, the error of TP is 0.14 kcal mol$^{-1}$ and the standard deviation is 0.28 kcal mol$^{-1}$, reflecting that the individual 1000 estimates have errors between −1.64 and

Table 2 Estimated free energies from numerical integration of eqn (5) (NI), as well as TP (eqn (1)) and CA (eqn (3)) based on 1000 random simulations with 10 million data points for the various distributions. All entries are in kcal mol$^{-1}$. The last column gives $\Pi$ for the sample. The reported uncertainties are standard deviations

| Distribution | $\sigma_{\Delta U}$ | $\Delta G_{NI}$ | $\Delta G_{TP}$ | $\Delta G_{CA}$ | $\Pi$ |
|---|---|---|---|---|---|
| Gaus | 0.50 | −0.21 | −0.21 ± 0.00 | −0.21 ± 0.00 | 4.37 ± 0.00 |
| | 1.00 | −0.84 | −0.84 ± 0.00 | −0.84 ± 0.00 | 3.53 ± 0.00 |
| | 2.00 | −3.36 | −3.35 ± 0.03 | −3.36 ± 0.00 | 1.86 ± 0.00 |
| | 3.00 | −7.55 | −7.41 ± 0.28 | −7.55 ± 0.00 | 0.17 ± 0.00 |
| Gumb_r | 0.50 | 0.06 | 0.06 ± 0.00 | 0.02 ± 0.00 | 4.46 ± 0.00 |
| | 1.00 | −0.09 | −0.09 ± 0.00 | −0.39 ± 0.00 | 3.86 ± 0.00 |
| | 2.00 | −0.79 | −0.79 ± 0.00 | −2.46 ± 0.00 | 2.82 ± 0.00 |
| Gumb_l | 0.50 | −0.56 | −0.56 ± 0.01 | −0.44 ± 0.00 | 4.15 ± 0.00 |
| | 1.00 | −4.17 | −4.13 ± 0.65 | −1.29 ± 0.00 | 0.17 ± 0.00 |
| Stud. t-10 | 1.12 | −7.12 | −4.15 ± 1.61 | −1.05 ± 0.00 | 0.32 ± 0.00 |
| Beta | 0.46 | 3.75 | 3.74 ± 0.00 | 3.77 ± 0.00 | 4.39 ± 0.00 |

Open Access Article. Published on 13 May 2024. Downloaded on 8/2/2025 6:55:55 AM. This article is licensed under a Creative Commons Attribution-NonCommercial 3.0 Unported Licence.

0.58 kcal mol$^{-1}$. $\Pi = 0.2$ suggests that the result is unreliable. Naturally, the CA result coincides with the numerical results, because eqn (3) is exact for a Gaussian distribution. With 10 million samples, the sample mean and variance are estimated very accurately with a standard deviation below 0.005 kcal mol$^{-1}$.

On the other hand, the results are different for the other distributions. For the three distributions with $\sigma_{\Delta U} \leq$ 0.5 kcal mol$^{-1}$ (Gumb0_r, Gumb0_l and Beta), TP gives excellent results, with errors of 0.01 kcal mol$^{-1}$ or less. The same applies also to the Gumb_r distributions with $\sigma_{\Delta U} = 1$ and 2 kcal mol$^{-1}$ $\Pi$ = 2.8–4.5 also indicates that the results are converged. However, for all these distributions, the performance of CA is worse, with errors of 0.02–0.12 kcal mol$^{-1}$ for the three distributions with $\sigma_{\Delta U} \leq$ 0.5 kcal mol$^{-1}$ and 0.3 kcal mol$^{-1}$ for Gumb_r with $\sigma_{\Delta U} = 1$ kcal mol$^{-1}$. Even worse, when the $\sigma_{\Delta U}$ value of Gumb_r increases to 2 kcal mol$^{-1}$, the error of CA becomes as high as 1.7 kcal mol$^{-1}$. This is not reflected by the standard deviation, which is always less than 0.005 kcal mol$^{-1}$ for CA.

For the remaining two distributions, Gumb_l with $\sigma_{\Delta U} =$ 1 kcal mol$^{-1}$ and Student *t*-10 with $\sigma_{\Delta U} = 1.12$ kcal mol$^{-1}$, the TP results are poor, with errors of 0.04–3 kcal mol$^{-1}$ and standard deviations of 0.6–1.6 kcal mol$^{-1}$ (indicating errors of up to 6.0 and 7.3 kcal mol$^{-1}$ in the 1000 individual simulations). The CA results are even worse, with errors of 2.9–6.1 kcal mol$^{-1}$, but the standard deviation is still less than 0.005 kcal mol$^{-1}$. $\Pi = 0.2$–0.3 indicates that the results are unreliable. Compared to the Gaussian distribution, both these two distributions have a higher probability of negative values. Owing to the exponential average in TP, the most negative $\Delta U$ values may lead to the numerical instability of the results. With finite samples, there is a large probability that the most negative values are over- or undersampled, which may have a strong impact on the result.

We also repeated these calculations with different sample sizes. The results in Fig. 3a show that for Gaussian distributions, the $\Delta G$ results of TP and CA are almost the same. Moreover, the CA results converge faster than the TP results, and this becomes more pronounced when $\sigma_{\Delta U}$ increases. With $\sigma_{\Delta U} = 2.0$, the convergence of TP is very slow, and it frequently gives too negative estimates of $\Delta G$.

For the two Gumbel distributions, there is a significant discrepancy between the results predicted by TP and CA, and the difference increases with $\sigma_{\Delta U}$. For the Gumb_r distribution, TP shows a faster convergence than CA, and CA always gives too negative (incorrect) predictions of $\Delta G$. For the Gumb_l distribution, the opposite is true: CA shows a faster convergence than TP, and it always gives a too positive (and still incorrect) prediction of $\Delta G$. For $\sigma_{\Delta U} = 1$ and 2 kcal mol$^{-1}$, TP shows a very slow convergence towards the correct result, with a very large range of the estimates and many occasionally too negative estimates, reflecting oversampling of negative values of $\Delta U$. This shows that for non-Gaussian distributions, the effects of the higher-order terms in the cumulant expansion cannot be neglected.

### The relation between $\Pi$ and $\sigma_{\Delta U}$

As discussed in the Introduction, both $\sigma_{\Delta U}$ and the Kofke $\Pi$ bias measure have often been used to check the convergence of single-step calculations. It is therefore of interest to know the relation between these two measures. If $\Delta U$ follows a Gaussian distribution, so that $\Delta G$ can be calculated from the second-order cumulant expansion (eqn (3)), then eqn (4) can be written as:

$$\Pi = \sqrt{W_{\mathrm{L}}\left[\frac{(N-1)^2}{2\pi}\right]} - \frac{\sigma_{\Delta U}}{k_{\mathrm{B}}T} \tag{11}$$

directly showing the relationship between $\Pi$ and $\sigma_{\Delta U}$. The first term depends only on the sample size $N$. Thus, for a fixed sample size, $\Pi$ is linearly related to $\sigma_{\Delta U}$ with a negative slope given by

$$\frac{\partial \Pi}{\partial \sigma} = -\frac{1}{k_{\mathrm{B}}T} \tag{12}$$

The relation is illustrated in Fig. 4. It can be seen that with a constant sample size, $\Pi$ decreases when $\sigma_{\Delta U}$ increases. Moreover, for a certain $\sigma_{\Delta U}$, $\Pi$ becomes larger when the sample size increases, but the rate of growth is slow.

For each value of $\sigma_{\Delta U}$ or $N$, we can set $\Pi$ to the limiting value of 0.5 and solve eqn (4) for the other variable. These solutions are shown in Fig. 5 (and some numerical values are given in Table S1 in the ESI†). For example, with 1000, 1 million, and 1 billion samples, $\sigma_{\Delta U}$ must be less than 1.6, 2.5, and 3.3 kcal mol$^{-1}$ for $\Pi$ to attain an acceptable value ($\geq$0.5). Conversely, $\sigma_{\Delta U}$ values of 1, 2, 3, and 4 kcal mol$^{-1}$ require 60, 16 thousand, 62 million, and $3.6 \times 10^{12}$ samples for convergence according to $\Pi \geq 0.5$. This shows that the limit of $\sigma_{\Delta U}$ depends on $N$ and should not be given without specifying $N$.

### Convergence of the various distributions

A problem with the $\Pi$ bias measure is that it does not indicate the accuracy of the calculated $\Delta G$ values. Therefore, we performed a number of numerical simulations with well-defined convergence limits. We tested three types of distributions, Gaussian, Gumb_l, and Gumb_r, and three $\sigma_{\Delta U}$ values, 0.5, 1.0, and 2.0 kcal mol$^{-1}$, which are below, within and out of the recommended range (0.6–1.2 kcal mol$^{-1}$). For each distribution, we performed numerical simulations with the aim to determine the minimum sample size ($N_{\min}$) required to achieve converged $\Delta G$. We consider $\Delta G$ converged when the calculated value falls within 0.5 kcal mol$^{-1}$ of the value obtained by numerical integration with a confidence of 95% (estimated by repeating the simulation 1000 times). This is similar to what has been used in earlier studies,[33,51] and the simulations can, of course, easily be repeated with other convergence criteria. When the minimum sample size required has been obtained, the corresponding $\Pi$ value was calculated according to eqn (4), using $\Delta G$ obtained from either TP, CA, or numerical integration. We repeated the simulations 100 times to obtain the uncertainty of all estimates. The results are listed in Table 3.

 © 2024 The Author(s). Published by the Royal Society of Chemistry

Open Access Article. Published on 13 May 2024. Downloaded on 8/2/2025 6:55:55 AM.
This article is licensed under a Creative Commons Attribution-NonCommercial 3.0 Unported Licence.

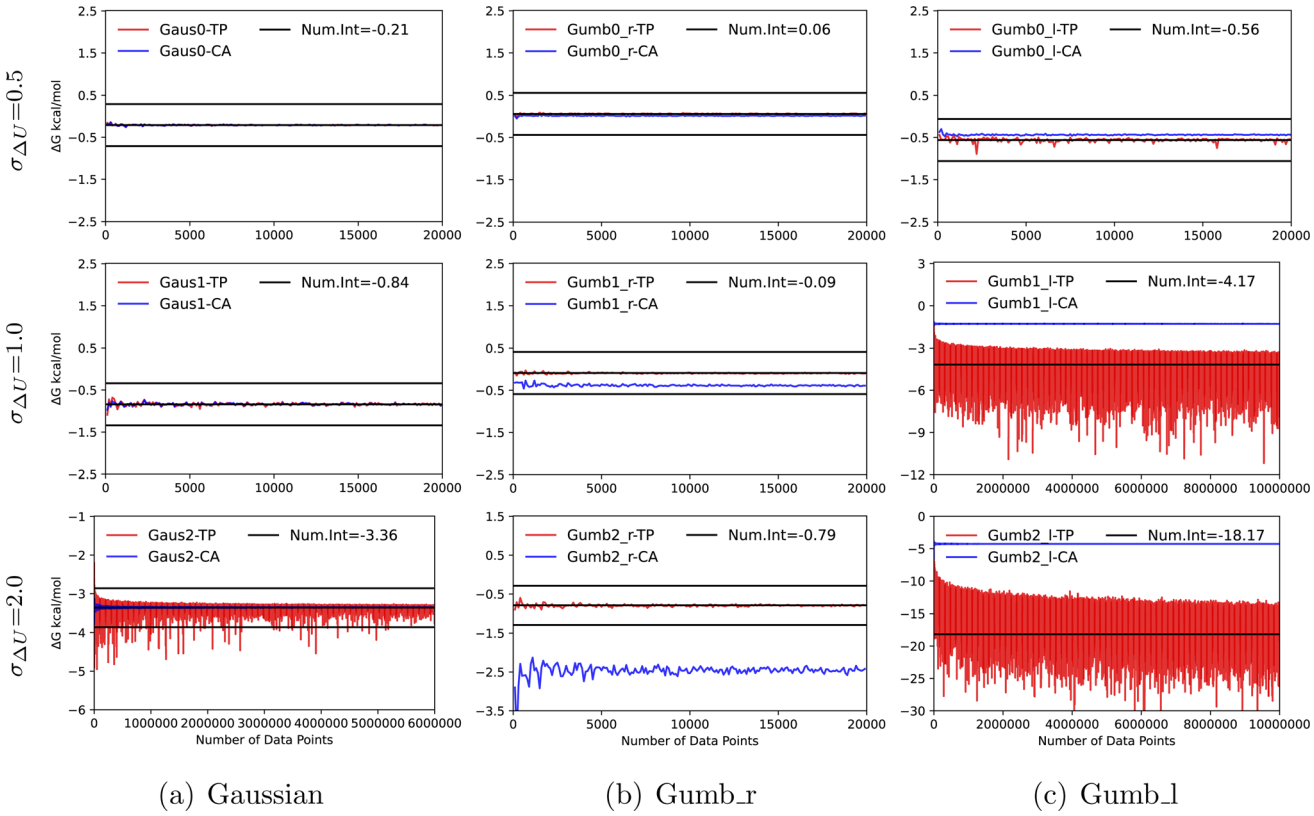


Fig. 3 $\Delta G$ estimated using different sample sizes. The solid black lines represent the numerical integration result, as well as an error range of $\pm 0.5$ kcal mol$^{-1}$. The calculated results with TP and CA are shown in red and blue curves, respectively. Results are shown for Gaussian, Gumb_r, and Gumb_l distributions (in the left (a), middle (b), and right columns (c), respectively). Three values of $\sigma_{\Delta U}$ are used: 0.5 (top), 1.0 (middle) and 2.0 (bottom).

From Table 3, it can be seen that when $\sigma_{\Delta U} = 0.5$, $N_{\min}$ for TP and CA is almost the same for each distribution. Gumb_r requires the smallest number of samples (4) and Gumb_l the largest sample size (11–14). Naturally, when $\sigma_{\Delta U}$ increases, $N_{\min}$ also increases. On the other hand, for Gaussian distributions with equal $\sigma_{\Delta U}$ values, $N_{\min}$ for CA is smaller than that for TP and the difference increases with $\sigma_{\Delta U}$. This reflects that CA converges faster than TP for Gaussian distributions, as was discussed before. On the other hand, for non-Gaussian distributions, TP requires less samples than CA. In fact, CA converges to an incorrect value (as we also saw before), which is outside our convergence criterion (0.5 kcal mol$^{-1}$) for both Gumble distributions when $\sigma_{\Delta U}$ is high (therefore, no results are given for CA in Table 3). With Gumb_l, very large values for $N_{\min}$ are required also with TP and the required sample size grows rapidly with $\sigma_{\Delta U}$. Going from $\sigma_{\Delta U} = 0.5$ to 0.8, the required sample size increase from 14 to over 3 million and with larger $\sigma_{\Delta U}$, we could not generate sufficient samples to reach convergence.

The corresponding $\Pi$ values are also listed in Table 3. Due to the fluctuation, there are small differences between $\Pi_{\mathrm{Av}}$ and $\Pi_{\mathrm{NI}}$. For TP, $\Pi_{\mathrm{Av}}$ is always slightly larger (more positive) than $\Pi_{\mathrm{NI}}$ (by up to 0.2). With CA and the Gumbel distributions, the opposite is sometimes true, and the difference is slightly larger (up to 0.3). For the Gaussian distributions, all $\Pi$ values are less than 0.5. This is especially pronounced for CA and larger values of $\sigma_{\Delta U}$ (*e.g.* $-0.5$ for Gaus2). This, of course, reflects that $\Pi$ was developed for TP and is unaware of what method is actually used to estimate $\Delta G$.

For the Gumb_r distribution with TP, $\Pi$ is always <0.5, reflecting that $\Pi$ and the convergence limit were developed assuming a Gaussian distribution. Since Gumb_r is skewed towards positive $\Delta U$ values, the TP convergence is faster than for a Gaussian distribution, and therefore, lower values of $\Pi$ are acceptable (*e.g.* $-0.2$ for $\sigma_{\Delta U} = 2$ kcal mol$^{-1}$). Conversely, the opposite is true for the Gumb_l distributions, which are skewed towards more negative values. Here, the limiting $\Pi$ value is 2.7 for $\sigma_{\Delta U} = 0.8$ kcal mol$^{-1}$. For CA, the results are the opposite because it converges towards incorrect estimates of $\Delta G$.

These results provide us with several interesting observations:

- The criterion for $\Pi$ implicitly involves some convergence and confidence thresholds. Those used by us (within 0.5 kcal mol$^{-1}$ of the correct result with 95% confidence) are slightly less strict for a Gaussian distribution than $\Pi \geq 0.5$.
- For CA and Gaussian distributions, less strict values for $\Pi$ can be used.
- The limit for $\Pi$ depends on the underlying distribution.
- CA is applicable for a Gaussian distribution but gives incorrect results for other distributions. The difference in $\Delta G$

Open Access Article. Published on 13 May 2024. Downloaded on 8/2/2025 6:55:55 AM.
This article is licensed under a Creative Commons Attribution-NonCommercial 3.0 Unported Licence.

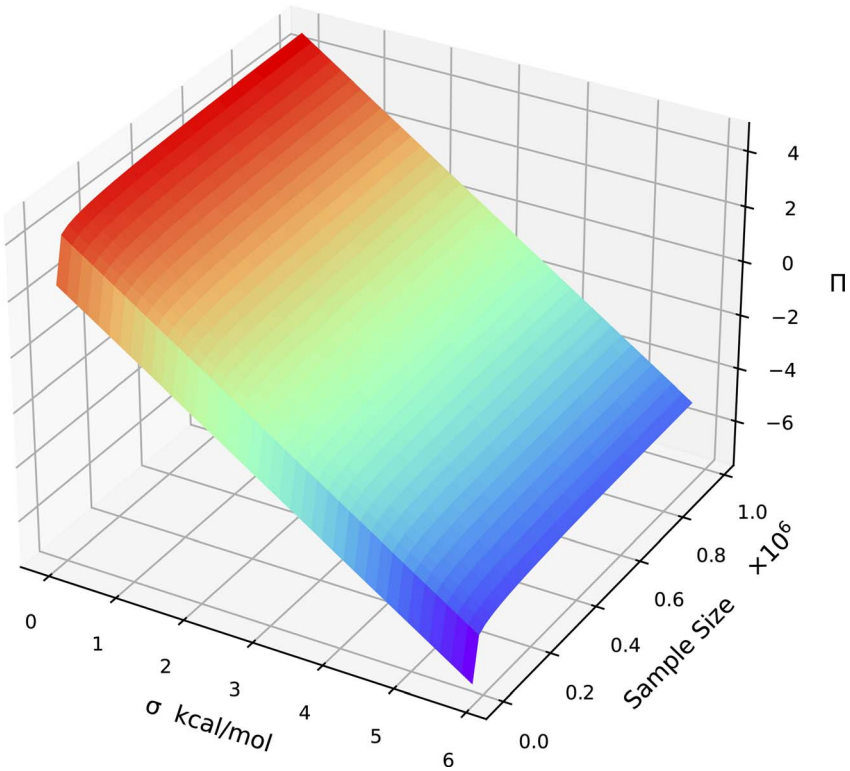


Fig. 4 Relation between the Π bias measure, $\sigma_{\Delta U}$ and the sample size $N$ for a Gaussian distribution.

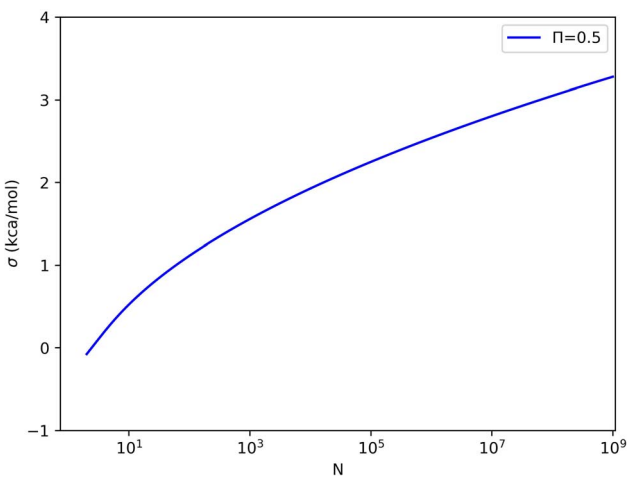


Fig. 5 Relation between $\sigma_{\Delta U}$ and the sample size $N$ when $\Pi = 0.5$.

estimated with CA and TP can used to decide whether the distribution is Gaussian or not.

### Reliability of $\Pi \geq 0.5$

In practical applications of the reference-potential method, the distribution and the reference value are unknown. The key question is to decide whether an obtained $\Delta G$ result is reliable or if additional energies should be sampled, *i.e.*, to decide the proper sample size. As mentioned several times, a frequently used criterion for convergence of TP is $\Pi \geq 0.5$. In this section, we evaluate whether we can use this criterion to decide the required sample size and how this can be done practically. We first tried the most natural approach, *i.e.*, to increase the number of samples until $\Pi \geq 0.5$. This was tested with numerical simulations using the same distributions as in the previous section. The simulations were repeated 1000 times for each of the distributions to gain confidence in the results.

The results in Table 4 show that, in general, it is not a good procedure to accept the $\Delta G$ value as soon as $\Pi \geq 0.5$, because this can happen by chance (because $\Pi$ depends on the calculated value of $\Delta G$). In fact, at least one of the 1000 individual simulations indicated that the results have converged already with three samples (the lowest number tested) for all distributions. As a consequence, only the three Gumb_r distributions (for which we know from the previous subsection that $\Pi \geq 0.5$ is too strict) and the Gaus0 distribution give $\Delta G$ results that are correct within 0.5 kcal mol$^{-1}$ in more than 95% of the simulations (conf. column in Table 4). For the two Gumb_l distributions, the problem is that $\Pi \geq 0.5$ is too loose. However, for the two Gaussian distributions, the problem is convergence by chance, and the problem is very serious as only 53 and 0.3% of the simulations give correct results within 0.5 kcal mol$^{-1}$ for $\sigma_{\Delta U} = 1$ or 2 kcal mol$^{-1}$, respectively.

Therefore, we tested to use larger thresholds. Unfortunately, it seems hard to suggest a threshold for $\Pi$ that works for all distributions. For example, $\Pi \geq 0.75$ works quite well for Gaus1, giving $\Delta G$ results that agree with the true value within 0.5 kcal mol$^{-1}$ more than 95% of the simulations and giving $N_{\min}$ values of 12–152 (average 77) that are similar to the value

 © 2024 The Author(s). Published by the Royal Society of Chemistry

Open Access Article. Published on 13 May 2024. Downloaded on 8/2/2025 6:55:55 AM. This article is licensed under a Creative Commons Attribution-NonCommercial 3.0 Unported Licence.

Table 3 The minimum sample size required to achieve convergence ($N_{min}$; *i.e.*, reproduce the numerical-integration result within 0.5 kcal mol$^{-1}$ with 95% confidence) in the numerical simulations of three distributions, each with three values of $\sigma_{\Delta U}$ (for Gumb_l, no convergence was obtained with up to 10 million samples for $\sigma_{\Delta U} > 0.9$)[a]

| | | TP | | | CA | | |
|---|---|---|---|---|---|---|---|
| Distribution | $\sigma_{\Delta U}$ kcal mol$^{-1}$ | $N_{min}^{AV}$ | $\Pi_{Av}$ | $\Pi_{NI}$ | $N_{min}^{AV}$ | $\Pi_{Av}$ | $\Pi_{NI}$ |
| Gaus | 0.5 | 5.4 ± 0.5 | 0.34 ± 0.04 | 0.19 ± 0.06 | 5.4 ± 0.5 | 0.32 ± 0.04 | 0.19 ± 0.05 |
| | 1.0 | 44.6 ± 2.3 | 0.46 ± 0.02 | 0.38 ± 0.02 | 35.7 ± 1.5 | 0.33 ± 0.02 | 0.29 ± 0.02 |
| | 2.0 | 5732 ± 291 | 0.30 ± 0.01 | 0.23 ± 0.01 | 370 ± 10 | −0.54 ± 0.01 | −0.55 ± 0.01 |
| Gumb_r | 0.5 | 3.5 ± 0.5 | 0.17 ± 0.07 | 0.00 ± 0.10 | 3.5 ± 0.5 | 0.12 ± 0.07 | −0.10 ± 0.10 |
| | 1.0 | 10.9 ± 0.7 | 0.16 ± 0.03 | 0.08 ± 0.03 | 135 ± 8 | 0.82 ± 0.02 | 1.13 ± 0.02 |
| | 2.0 | 54.9 ± 2.4 | −0.19 ± 0.02 | −0.24 ± 0.02 | | | |
| Gumb_l | 0.5 | 14.2 ± 1.2 | 0.71 ± 0.03 | 0.50 ± 0.04 | 11.4 ± 0.8 | 0.68 ± 0.03 | 0.39 ± 0.04 |
| | 0.8 | 3 106 100 ± 85 600 | 2.68 ± 0.01 | 2.49 ± 0.01 | | | |

[a] The corresponding values of Π at $N_{min}$ are also given, using $\Delta G$ either from the simulation ($\Pi_{Av}$) or from numerical integration ($\Pi_{NI}$). The simulations were repeated 100 times, and the reported precision is the standard deviation over these 100 repeats (thus, the standard error is 10 times smaller).

Table 4 Number of conformations needed to obtain $\Pi \geq 0.5$ ($N_{min}$) in numerical simulations using different distributions with different values of $\sigma_{\Delta U}$. For each distribution, 1000 individual simulations were performed and in each simulation, the number of samples was increased by one until $\Pi \geq 0.5$. The table lists the average, lower, and upper limits of $N_{min}$ in these simulations, as well as the average of Π, the percentage of the simulations that give $\Delta G$ within 0.5 kcal mol$^{-1}$ of the reference value from numerical integration (conf.), and the average deviation of the calculated $\Delta G$ from this value ($\Delta\Delta G_{Av}$, in kcal mol$^{-1}$)

| | $N_{min}$ | | | | | |
|---|---|---|---|---|---|---|
| Distribution | Av | Low | Up | $\Pi_{Av}$ | Conf. % | $\Delta\Delta G_{Av}$ |
| Gaus0 | 6 | 3 | 12 | 0.63 | 96 | 0.13 |
| Gaus1 | 18 | 3 | 43 | 0.61 | 53 | 0.52 |
| Gaus2 | 4030 | 3 | 5425 | 0.52 | 0.3 | 0.71 |
| Gumb0_r | 6 | 3 | 10 | 0.63 | 100 | 0.01 |
| Gumb1_r | 13 | 3 | 29 | 0.61 | 95 | 0.08 |
| Gumb2_r | 229 | 3 | 338 | 0.53 | 98 | 0.17 |
| Gumb0_l | 6 | 3 | 11 | 0.65 | 75 | 0.38 |
| Gumb1_l | 16 | 3 | 47 | 0.63 | 0 | 3.67 |

(45) listed in Table 3. However, for Gaus2, this threshold gives $N_{min}$ values that are much too large: Even the lower limit is 2.5 times larger than the value in Table 3 (14 402 compared to 5732 ± 29; note that we here used the standard error, rather than the standard deviation given in Table 3).

Third, we instead required that $\Pi \geq 0.5$ a certain number of consecutive times ($n_{times}$) before $\Delta G$ is accepted. The results for $n_{times}$ ranging from 2 to 5 are listed in Table 5. It can be seen that for the two Gaussian distributions, $n_{times} = 4$ seems to be appropriate – it gives results that are within 0.5 kcal mol$^{-1}$ of the reference result 96% of the simulations (conf. in Table 5), whereas the corresponding confidence for $n_{times} = 3$ is only 89–94%. For the Gaus1 distribution, the average number of samples needed for convergence ($N_{min}$(Av) = 56 in Table 5) is only slightly larger than the value reported in Table 3 (45 ± 0.2). However, for Gaus2 even the lowest $N_{min}$ (6455) is larger than the value reported in Table 3 (5732 ± 29).

For the Gumbel distribution, we obtain the expected results: Gumb_r always gives a very high confidence, 99–100%, because $\Pi \geq 0.5$ is too strict, whereas Gumb1_l always gives a confidence of 0%, because $\Pi \geq 0.5$ is too floppy (but Gumb0_l actually gives a confidence of 98% for $n_{times} = 4$, simply because the variance is so small).

## A practical procedure

The results in the previous section show that the limit of Π involves some implicit convergence limits and that it is hard to suggest proper limits that are valid for different distributions. Therefore, we in this section suggest another more practical procedure. It is based on numerical simulations of Gaussian distributions with different values of $\sigma_{\Delta U}$, the results of which are presented in Table 6. For different values of $\sigma_{\Delta U}$, the minimum sample size $N_{min}$ needed to converge $\Delta G$ within 0.5 kcal mol$^{-1}$ of the reference value (from numerical integration) with a confidence of 95% over 1000 samples was estimated (as in Table 3). This was done both for TP and CA. The simulations were repeated 100 times to get uncertainties of $N_{min}$. For each value of $N_{min}$, we also estimated the average value of Π. In addition, we estimated the mean of the weight of the largest term in the average in eqn (1), $w_{max}$, as well as the mean absolute difference in $\Delta G$ calculated with TP or CA, $\Delta\Delta G_{CA}$. Both can be used to decide whether the distribution is Gaussian or not.

From the results in Table 6, it can be seen that $w_{max}$ estimated at $N_{min}$ for TP decreases slowly with $\sigma_{\Delta U}$, from 0.40 for $\sigma_{\Delta U} = 0.5$ kcal mol$^{-1}$ to 0.22 for $\sigma_{\Delta U} = 3.0$ kcal mol$^{-1}$, which is at the practical upper limit for obtaining converged free energies with TP. At the same time, $\Delta\Delta G_{CA}$ increases from 0.01 to 0.17 kcal mol$^{-1}$. Fig. 6 shows histograms for $w_{max}$ for Gumb_r, Gaussian, and Gumb_l distributions with the same $\sigma_{\Delta U}$ = 1.0 kcal mol$^{-1}$. It can be seen that Gumb_r gives the lowest values and Gumb_l the highest values. Thus, $w_{max}$ may give an indication of the type of distribution.

Based on these results, we suggest the following practical procedure for $\Delta G$ estimated with the reference-potential method:

Open Access Article. Published on 13 May 2024. Downloaded on 8/2/2025 6:55:55 AM.
This article is licensed under a Creative Commons Attribution-NonCommercial 3.0 Unported Licence.

Table 5 Number of conformations ($N_{min}$) needed to obtain $\Pi \geq 0.5$ $n_{times}$ times in a row in numerical simulations using different distributions with different values of $\sigma_{\Delta U}$[a]

| $n_{times}$ | Distribution | $N_{min}$ Av | Low | Up | $\Pi_{Av}$ | Conf. % | $\Delta\Delta G_{Av}$ kcal mol$^{-1}$ |
|---|---|---|---|---|---|---|---|
| 2 | Gaus1 | 36 | 9 | 61 | 0.20 | 83 | 0.31 |
| | Gaus2 | 6444 | 3971 | 7919 | 0.09 | 51 | 0.50 |
| | Gumb1_r | 22 | 4 | 39 | 0.64 | 99 | 0.04 |
| | Gumb2_r | 347 | 219 | 428 | 0.54 | 100 | 0.09 |
| | Gumb0_l | 9 | 4 | 17 | 0.71 | 90 | 0.28 |
| | Gumb1_l | 46 | 5 | 130 | 0.66 | 0 | 3.26 |
| 3 | Gaus1 | 47 | 7 | 76 | 0.20 | 94 | 0.22 |
| | Gaus2 | 8031 | 4969 | 9506 | 0.09 | 89 | 0.41 |
| | Gumb1_r | 29 | 6 | 43 | 0.66 | 99 | 0.03 |
| | Gumb2_r | 405 | 267 | 494 | 0.55 | 100 | 0.06 |
| | Gumb0_l | 12 | 5 | 26 | 0.78 | 94 | 0.23 |
| | Gumb1_l | 89 | 11 | 222 | 0.69 | 0 | 3.00 |
| 4 | Gaus1 | 56 | 21 | 85 | 0.19 | 96 | 0.18 |
| | Gaus2 | 9105 | 6455 | 10 616 | 0.10 | 96 | 0.36 |
| | Gumb1_r | 32 | 16 | 49 | 0.68 | 100 | 0.02 |
| | Gumb2_r | 440 | 307 | 539 | 0.56 | 100 | 0.05 |
| | Gumb0_l | 14 | 6 | 27 | 0.81 | 98 | 0.19 |
| | Gumb1_l | 140 | 19 | 352 | 0.70 | 0 | 2.82 |
| 5 | Gaus1 | 63 | 27 | 100 | 0.19 | 98 | 0.15 |
| | Gaus2 | 10 006 | 6966 | 11 971 | 0.11 | 98 | 0.32 |
| | Gumb1_r | 36 | 17 | 51 | 0.69 | 100 | 0.01 |
| | Gumb2_r | 468 | 353 | 554 | 0.56 | 100 | 0.04 |
| | Gumb0_l | 17 | 8 | 35 | 0.86 | 98 | 0.17 |
| | Gumb1_l | 203 | 29 | 512 | 0.71 | 0 | 2.28 |

[a] The entries are the same as in Table 4.

Table 6 The minimum sampling size ($N_{min}$) required to achieve convergence ($\Delta G$ estimated within 0.5 kcal mol$^{-1}$ of the reference value with 95% confidence over 1000 samples) in numerical simulations of Gaussian distributions with different values of $\sigma_{\Delta U}$, using both TP and CA[a]

| | TP | | | | CA | | | |
|---|---|---|---|---|---|---|---|---|
| $\sigma_{\Delta U}$ kcal mol$^{-1}$ | $N_{min}$ | $\Pi_{Av}$ | $w_{max}$ | $\Delta\Delta G_{CA}$ | $N_{min}$ | $\Pi_{Av}$ | $w_{max}$ | $\Delta\Delta G_{CA}$ |
| 0.50 | 5.4 ± 0.5 | 0.34 ± 0.04 | 0.40 ± 0.02 | 0.01 ± 0.00 | 5.4 ± 0.5 | 0.32 ± 0.04 | 0.40 ± 0.02 | 0.01 ± 0.00 |
| 0.75 | 15.8 ± 0.9 | 0.45 ± 0.02 | 0.31 ± 0.01 | 0.03 ± 0.00 | 15.4 ± 0.8 | 0.40 ± 0.02 | 0.31 ± 0.01 | 0.03 ± 0.00 |
| 1.00 | 44.6 ± 2.3 | 0.46 ± 0.02 | 0.27 ± 0.01 | 0.04 ± 0.00 | 35.7 ± 1.5 | 0.33 ± 0.02 | 0.30 ± 0.01 | 0.05 ± 0.00 |
| 1.25 | 125 ± 6 | 0.42 ± 0.01 | 0.26 ± 0.01 | 0.07 ± 0.01 | 72.4 ± 2.6 | 0.18 ± 0.01 | 0.31 ± 0.01 | 0.09 ± 0.01 |
| 1.50 | 380 ± 16 | 0.37 ± 0.01 | 0.25 ± 0.01 | 0.09 ± 0.01 | 134 ± 5 | −0.03 ± 0.01 | 0.34 ± 0.01 | 0.14 ± 0.01 |
| 1.75 | 1277 ± 48 | 0.32 ± 0.01 | 0.25 ± 0.01 | 0.11 ± 0.01 | 228 ± 8 | −0.27 ± 0.01 | 0.37 ± 0.01 | 0.23 ± 0.01 |
| 2.00 | 5732 ± 290 | 0.30 ± 0.01 | 0.24 ± 0.01 | 0.12 ± 0.01 | 370 ± 10 | −0.54 ± 0.01 | 0.40 ± 0.01 | 0.35 ± 0.01 |
| 2.25 | 24 900 ± 1150 | 0.24 ± 0.01 | 0.23 ± 0.00 | 0.14 ± 0.01 | 565 ± 16 | −0.83 ± 0.01 | 0.43 ± 0.01 | 0.52 ± 0.02 |
| 2.50 | 128 200 ± 5500 | 0.20 ± 0.01 | 0.23 ± 0.01 | 0.16 ± 0.01 | 836 ± 24 | −1.13 ± 0.01 | 0.46 ± 0.01 | 0.73 ± 0.02 |
| 2.75 | 949 000 ± 4500 | 0.19 ± 0.00 | 0.22 ± 0.01 | 0.16 ± 0.01 | 1247 ± 31 | −1.43 ± 0.01 | 0.49 ± 0.01 | 1.00 ± 0.02 |
| 3.00 | 7 489 200 ± 22 000 | 0.18 ± 0.00 | 0.22 ± 0.01 | 0.17 ± 0.01 | 1715 ± 52 | −1.76 ± 0.01 | 0.51 ± 0.01 | 1.34 ± 0.02 |
| 3.5 | | | | | 3091 ± 87 | −2.44 ± 0.01 | 0.56 ± 0.01 | 2.22 ± 0.03 |
| 4.0 | | | | | 45 130 ± 140 | −3.15 ± 0.01 | 0.60 ± 0.01 | 3.41 ± 0.03 |
| 5.0 | | | | | 12 700 ± 360 | −4.60 ± 0.01 | 0.66 ± 0.01 | 6.76 ± 0.04 |
| 10.0 | | | | | 203 000 ± 2700 | −12.35 ± 0.00 | 0.81 ± 0.01 | 45.7 ± 0.8 |
| 15.0 | | | | | 984 900 ± 12 800 | −20.41 ± 0.00 | 0.87 ± 0.01 | 124.0 ± 0.1 |
| 20.0 | | | | | 3 306 900 ± 7700 | −28.57 ± 0.00 | 0.89 ± 0.00 | 242.6 ± 0.2 |
| 25.0 | | | | | 7 698 000 ± 172 000 | −36.80 ± 0.00 | 0.91 ± 0.00 | 402.5 ± 0.2 |

[a] The corresponding values of $w_{max}$, $\Pi$, and $\Delta\Delta G_{CA}$ calculated for $N_{min}$ samples are also given. For each value of $\sigma_{\Delta U}$, 100 independent simulations with different random seeds were performed to obtain averages and uncertainties of all the calculated values. The uncertainties are standard deviations over these 100 simulations (thus, the standard errors are 10 times smaller).

 © 2024 The Author(s). Published by the Royal Society of Chemistry

Open Access Article. Published on 13 May 2024. Downloaded on 8/2/2025 6:55:55 AM.
This article is licensed under a Creative Commons Attribution-NonCommercial 3.0 Unported Licence.

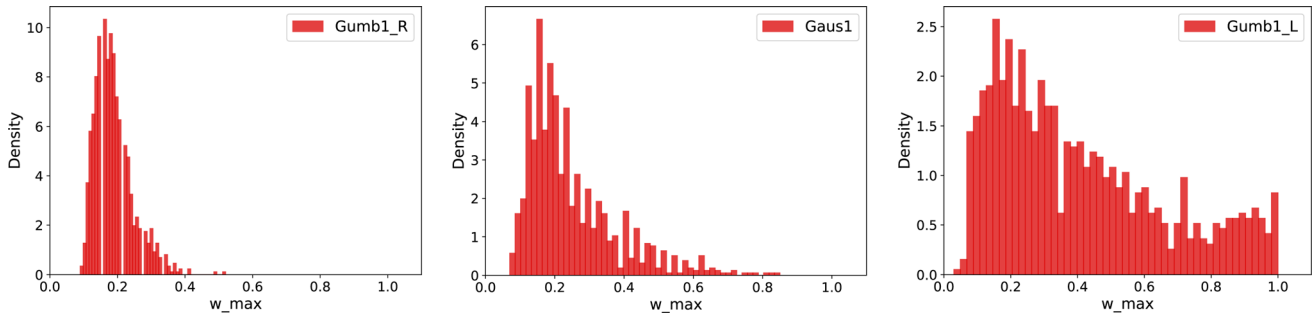


Fig. 6 Histograms of the $w_{max}$ for three distributions with $\sigma_{\Delta U} = 1.0$ kcal.

1. Sample $N_{start}$ samples and calculate $\sigma_{\Delta U}$. In the following, we used $N_{start} = 200$.

2. Read $N = N_{min}^{CA}$ for this value of $\sigma_{\Delta U}$ from Table 6 and obtain this number of samples.

3. Use a standard normality test to decide whether the distribution is Gaussian or not. We used the Shapiro–Wilk test and a $p$-value of 0.05 to decide if the sample is Gaussian.

4. If the distribution is not Gaussian, read $N = N_{min}^{TP}$ from Table 6. If $\sigma_{\Delta U}$ is larger than the tabulated values, use $N = N_{max}$, which was set to $1 \times 10^7$ in this study. If the distribution is Gaussian, no additional samples are needed.

5. Obtain $N$ samples and calculate $\sigma_{\Delta U}$, $\Delta G$ with both CA and TP, as well as $w_{max}$ and $\Delta\Delta G_{CA}$. Calculate also the corresponding standard errors with bootstrapping (allowing for repeated samples).

6. Check that $\sigma_{\Delta U}$ has not increased significantly. If so, go back to 2. Also check that the normality test still gives the same result.

7. If the distribution is Gaussian, use $\Delta G$ from CA.

8. If the distribution is non-Gaussian, use $\Delta G$ from TP.

9. If $w_{max}$ + SE is less than $w_{max}$ from Table 6 and SE is the standard error from 1000 samples of bootstrapping, the estimated $\Delta G$ is deemed to be reliable; otherwise it is deemed that no reliable results can be obtained (the distribution is too much skewed towards negative values).

This procedure is based on the results in Table 6 and therefore on the convergence criteria used there ($\Delta G$ should reproduce the reference results within 0.5 kcal mol$^{-1}$ in 95% of the simulations). If a user is interested in other (*e.g.* more strict) criteria, a new table could easily be constructed with our programs. The advantage with our criteria, in contrast to the criterion that $\Pi \geq 0.5$, is that they have an easy-to-interpret meaning in terms of reproducing correct results and therefore they can immediately be adapted to the need of the user.

We have tested this procedure for three different distributions (Gaussian, Gumb_r and Gumb_l) and 2–4 values of $\sigma_{\Delta U}$. For each distribution and $\sigma_{\Delta U}$, we followed the procedure 1000 times and count how many times the procedure yielded a $\Delta G$ that was judged reliable and also was within the numerical result within 0.5 kcal mol$^{-1}$ (true positive, TP) or a $\Delta G$ that judged unreliable and it was not within 0.5 kcal mol$^{-1}$ of the numerical results (true negative, TN).

From the results in Table 7, it can be seen that the Shapiro–Wilk test correctly identify the Gaussian and non-Gaussian distributions with an accuracy of 95–100%. For the Gaussian and Gumb_r distributions, we obtain the correct $\Delta G$ value within 0.5 kcal mol$^{-1}$ in 94–100% of the simulations, with average values that are within 0.02 kcal mol$^{-1}$ of the numerical reference. For the Gumb_l distribution, we judge that 91–92% of the results are not reliable, but for the distributions with $\sigma_{\Delta U}$ = 0.75 kcal mol$^{-1}$, many of the $\Delta G$ values are still within 0.5 kcal mol$^{-1}$ of the numerical results, giving a TP + TN confidence of only 75%, whereas with $\sigma_{\Delta U} = 1.5$ kcal mol$^{-1}$, the proportion of correct predictions increases to 91%. The problem with the former distribution is that much too few $\Delta U$ values are sampled, giving too positive estimates of $\Delta G$. However, occasionally, unusually negative $\Delta U$ values are obtained, which happen to give $\Delta G$ within the convergence limit, *i.e.* a cancellation of two errors. It should also be noted that for the Gumb_l distribution, the simulations with a restricted number of samples, $\sigma_{\Delta U}$ calculated from the sample may be quite different from the analytical value of $\sigma_{\Delta U}$ (the difference is not significant for the other two distributions) and if we restrict the investigation to samples that give a correct $\sigma_{\Delta U}$ (within 0.005 kcal mol$^{-1}$), the successful (TP + TN) predictions increase to 81 and 93% for the Gumb_l distributions with $\sigma_{\Delta U} = 0.75$ and 1.5 kcal mol$^{-1}$, respectively. Thus, Gumb_l and other distributions with a skew towards left remain problematic for reference-potential approaches.

Finally, we also performed an application with data from a practical example of a single-step QM perturbation. We employed data from our previous study of the binding of cyclic carboxylate ligands to the octa-acid deep-cavity host using semiempirical (SQM) and density functional theory (DFT) methods.[25] We considered four ligands, benzoate (Bz), *para*-methyl-benzoate (MeBz), *para*-ethyl-benzoate (EtBz) and *meta*-chloride-benzoate (mClBz) and the free energy change of going from SQM to DFT based on up to 5000 snapshots from a SQM/MM molecular dynamics simulation, either for the ligands free in water solution or when bound to the octa-acid host. We followed the procedure suggested in this section and the results are collected in Table 8.

It can be seen that for all four ligands in both surroundings, $\sigma_{\Delta U}$ is rather small, 1.3–1.9 kcal mol$^{-1}$. Likewise, all distributions of $\Delta U$ are Gaussian (four examples are shown in Fig. S2†).

Open Access Article. Published on 13 May 2024. Downloaded on 8/2/2025 6:55:55 AM.
This article is licensed under a Creative Commons Attribution-NonCommercial 3.0 Unported Licence.

Table 7 Test of the suggested approach for statistical distributions[a]

| Distribution | $\sigma_{\Delta U}$ | $\Delta G_{NI}$ | $N_{min}^{CA}$ | Gaus? | $N_{min}^{TP}$ | $w_{max}$ | $\Delta G$ | % $R$ | TP + TN | Conf. |
|---|---|---|---|---|---|---|---|---|---|---|
| Gaussian | 0.75 | −0.47 | 200 | 95% | | | −0.47 ± 0.07 | 5% | 100% | 100% |
| Gaussian | 1.50 | −1.89 | 200 | 95% | | | −1.86 ± 0.07 | 4% | 97% | 97% |
| Gaussian | 2.50 | −5.24 | 836 | 96% | | | −5.21 ± 0.06 | 3% | 92% | 93% |
| Gaussian | 3.00 | −7.55 | 1715 | 95% | | | −7.54 ± 0.06 | 4% | 93% | 94% |
| Gumb_r | 0.75 | 0.008 | 200 | 0% | 200 | 0.03 ± 0.01 | 0.01 ± 0.02 | 100% | 100% | 100% |
| Gumb_r | 1.50 | −0.39 | 200 | 0% | 380 | 0.05 ± 0.01 | −0.38 ± 0.07 | 100% | 100% | 100% |
| Gumb_r | 2.50 | −1.27 | 836 | 0% | 128 290 | 0.00 ± 0.00 | −1.28 ± 0.01 | 100% | 100% | 100% |
| Gumb_r | 3.00 | −1.82 | 1715 | 0% | 7 502 341 | 0.00 ± 0.00 | −1.83 ± 0.00 | 100% | 100% | 100% |
| Gumb_l | 0.75 | −1.73 | 200 | 0% | 200 | 0.19 ± 0.11 | −1.09 ± 0.31 | 8% | 75% | 17% |
| Gumb_l | 1.50 | −9.77 | 200 | 0% | 380 | 0.44 ± 0.13 | −4.10 ± 0.98 | 9% | 91% | 0% |

[a] We used three different distributions with 2–4 different values of $\sigma_{\Delta U}$. The third column gives the target value ($\Delta G_{NI}$ in kcal mol$^{-1}$) from numerical integration. We followed the procedure described in the text. The fourth column shows either $N_{min}^{CA}$ for this value of $\sigma_{\Delta U}$ from Table 6 or $N_{start} = 200$ if it is larger. The fifth column shows the results of the normality test. If it was considered to be Gaussian, the $\Delta G_{CA}$ result was accepted (shown in the eighth column). Otherwise, $N_{min}^{TP}$ samples were used (from Table 6 or $N_{start} = 200$ if it is still larger; shown in the sixth column) and $w_{max}$ and $\Delta G_{TP}$ were calculated. $w_{max}$ was compared to what is expected for a Gaussian distribution with this number of samples (from Table 6 or from Table S2 with $N_{start} = 200$) and based on this, the results were deemed reliable ($R$ in column eight) or unreliable. The ninth column shows the percentage of true positive and true negative (TP + TN) when the approach was tested 1000 times for each distribution (all values in the table are averages over these 1000 repeats). The last column (conf.) shows the percentage of samples giving correct results within 0.5 kcal mol$^{-1}$.

Table 8 Application of our suggested approach to the calculation of SQM → DFT $\Delta G$ for four ligands binding to the octa-acid host (kcal mol$^{-1}$). Values marked with "All" employs all 5000 snapshots employed in the original study.[25] Gaus? indicates whether the distribution was considered Gaussian

| Ligand | Surrounding | $\sigma_{\Delta U}^{N_{start}}$ | $\sigma_{\Delta U}^{All}$ | $N_{min}^{CA}$ | Gaus? | $\Delta G_{CA}^{N_{min}^{CA}}$ | $\Delta G_{CA}^{All}$ | $\Delta G_{TP}^{All}$ |
|---|---|---|---|---|---|---|---|---|
| Bz | bound | 1.30 | 1.30 | 134 | Y | −4.02 | −3.79 | −4.05 |
| | unbound | 1.67 | 1.59 | 228 | Y | −5.39 | −5.58 | −6.07 |
| MeBz | bound | 1.86 | 1.81 | 370 | Y | −2.18 | −2.64 | −2.70 |
| | unbound | 1.91 | 1.84 | 370 | Y | −5.48 | −5.29 | −5.42 |
| EtBz | bound | 1.77 | 1.83 | 370 | Y | −3.21 | −3.47 | −3.67 |
| | unbound | 1.88 | 1.84 | 370 | Y | −5.59 | −5.29 | −5.28 |
| mClBz | bound | 1.33 | 1.37 | 134 | Y | −3.89 | −3.90 | −4.06 |
| | unbound | 1.70 | 1.66 | 228 | Y | −6.01 | −6.31 | −7.29 |

Therefore, we can employ CA to calculate $\Delta G$ and 134–370 snapshots are enough to obtain results converged to within 0.5 kcal mol$^{-1}$. The resulting $\Delta G$ values are shown in Table 8. It can be seen that they agree with the previously published CA results (based on all available 5000 snapshots) within 0.5 kcal mol$^{-1}$, *i.e.* within our target accuracy of 0.5 kcal mol$^{-1}$. The agreement with the previously published TP results is worse, with deviations of up to 1.3 kcal mol$^{-1}$, but that mainly reflect that the TP results are not converged (with 5000 samples, $\Pi$ for unbound mClBz is only 0.2),[25] but it might also reflect small deviations of the data from Gaussian (the old CA and TP results show similar deviations). Thus, we can conclude that our suggested approach works well also with real computational data.

## Conclusions

In this paper, we discuss how the reliability of single-step exponential averaging (TP) can be judged. In particular, we discuss Wu and Kofke's bias measure $\Pi \geq 0.5$ and its relation to $\sigma_{\Delta U}$. We show that for Gaussian distributions, they follow the simple relation in eqn (12), as is illustrated in Fig. 4. For Gaussian distributions, $\Pi \geq 0.5$ works fine as a convergence criterion for $\Delta G$ estimated by TP and it is slightly stricter than requiring that the estimated $\Delta G$ should reproduce the correct results within 0.5 kcal mol$^{-1}$ with 95% confidence. However, for Gaussian distributions, CA is a more effective method to estimate $\Delta G$, converging much faster with respect to the number of samples.

Likewise, for distributions that are skewed more to the right than Gaussian distributions (more positive values of $\Delta U$; *e.g.* Gumb_r), $\Pi \geq 0.5$ is too strict, as are other convergence criteria based on Gaussian distributions. Therefore, TP shows a good convergence and gives accurate estimates of $\Delta G$, whereas CA gives incorrect estimates. Conversely, for distributions that skewed more to the left than Gaussian distributions (more negative values; *e.g.* Gumb_l), $\Pi \geq 0.5$ is too floppy. CA still gives incorrect estimates, whereas the TP estimates converge towards the correct value, but for $\sigma_{\Delta U} \geq 1$ kcal mol$^{-1}$, it becomes practically impossible to converge the results. Moreover, a direct application of the $\Pi \geq 0.5$ criterion may be

 © 2024 The Author(s). Published by the Royal Society of Chemistry

Open Access Article. Published on 13 May 2024. Downloaded on 8/2/2025 6:55:55 AM. This article is licensed under a Creative Commons Attribution-NonCommercial 3.0 Unported Licence.

problematic in practical applications, owing to the risk of obtaining $\Pi \geq 0.5$ by chance.

Therefore, we have instead suggested a practical procedure to judge the convergence of reference-potential calculations. It is based on $\sigma_{\Delta U}$ to estimate the number of samples needed for convergence, a Shapiro–Wilk test to decide whether the distribution is Gaussian or not, and $w_{\max}$ to decide whether a non-Gaussian distribution is skewed to the left or to the right. Using a set of distributions, we show that the approach works reasonably well. It also works well for a set of practical applications of SQM→DFT perturbations. However, distributions that are skewed towards negative values remain a challenge to converge with TP methods. In the future, it would be interesting to see if a similar approach can be used for nonequilibrium methods based on Jarzynski's equality,[52,53] which also involves an exponential average.

## Data availability

All data are available in the article, in the ESI† and from the authors upon request.

## Author contributions

MW performed all calculations, wrote the first version of the article and contributed to the editing of the final version. YM contributed to the editing of the final version of the manuscript. UR designed the work, contributed to the analysis of the data and to the editing of the final version of the manuscript.

## Conflicts of interest

There are no conflicts to declare.

## Acknowledgements

We thank Stefan Boresch and Marcos Verissimo Alves for their kind support. U. R. was supported by grants from the Swedish Research Council (project 2022-04978). M. W. was supported by the China Scholarship Council (No. 202108410209), the Educational Committee of Henan Province (23A150007), and the National Natural Science Foundation of China (No. 22303076). Y. M. was supported by the Oriental Scholar Program from the Shanghai Municipal Education Commission and the National Natural Science Foundation of China (Grant No. 22073030). Computer resources were provided by the National Academic Infrastructure for Supercomputing in Sweden (NAISS) and the Swedish National Infrastructure for Computing (SNIC) at Lunarc at Lund University.

## References

1 N. Homeyer and H. Gohlke, *In Silico Drug Discovery and Design*, 2013, pp 50–63.
2 W. L. Jorgensen and L. L. Thomas, Perspective on Free-Energy Perturbation Calculations for Chemical Equilibria, *J. Chem. Theory Comput.*, 2008, **4**, 869–876.
3 C. D. Christ, A. E. Mark and W. F. van Gunsteren, Basic Ingredients of Free Energy Calculations: A Review, *J. Comput. Chem.*, 2010, **31**, 1569–1582.
4 A. S. J. S. Mey, B. K. Allen, H. E. B. Macdonald, J. D. Chodera, D. F. Hahn, M. Kuhn, J. Michel, D. L. Mobley, L. N. Naden, S. Prasad, A. Rizzi, J. Scheen, M. R. Shirts, G. Tresadern and H. Xu, Best Practices for Alchemical Free Energy Calculations [Article v1.0], *Living J. Comp. Mol. Sci.*, 2020, **2**, 18378.
5 D. M. York, Modern Alchemical Free Energy Methods for Drug Discovery Explained, *ACS Phys. Chem. Au*, 2023, **3**, 478–491.
6 P. S. Nerenberg and T. Head-Gordon, New Developments in Force Fields for Biomolecular Simulations, *Curr. Opin. Struct. Biol.*, 2018, **49**, 129–138.
7 Z. Jing, C. Liu, S. Y. Cheng, R. Qi, B. D. Walker, J. P. Piquemal and P. Ren, Polarizable Force Fields for Biomolecular Simulations: Recent Advances and Applications, *Annu. Rev. Biophys.*, 2019, **48**, 371–394.
8 V. S. Inakollu, D. P. Geerke, C. N. Rowley and H. Yu, Polarisable Force Fields: What Do They Add in Biomolecular Simulations?, *Curr. Opin. Struct. Biol.*, 2020, **61**, 182–190.
9 J. Cheng, X. Liu, J. VandeVondele, M. Sulpizi and M. Sprik, Redox Potentials and Acidity Constants from Density Functional Theory Based Molecular Dynamics, *Acc. Chem. Res.*, 2014, **47**, 3522–3529.
10 U. Ryde and P. Söderhjelm, Ligand-Binding Affinity Estimates Supported by Quantum-Mechanical Methods, *Chem. Rev.*, 2016, **116**, 5520–5566.
11 F. L. Kearns, P. S. Hudson, S. Boresch and H. L. Woodcock, Methods for Efficiently and Accurately Computing Quantum Mechanical Free Energies for Enzyme Catalysis, *Methods Enzymol.*, 2016, **577**, 75–104.
12 J. Kästner, H. M. Senn, S. Thiel, N. Otte and W. Thiel, QM/MM Free-Energy Perturbation Compared to Thermodynamic Integration and Umbrella Sampling: Application to an Enzymatic Reaction, *J. Chem. Theory Comput.*, 2006, **2**, 452–461.
13 M. Wang, Y. Mei and U. Ryde, Predicting Relative Binding Affinity Using Nonequilibrium QM/MM Simulations, *J. Chem. Theory Comput.*, 2018, **14**, 6613–6622.
14 V. Vennelakanti, A. Nazemi, R. Mehmood, A. H. Steeves and H. J. Kulik, Harder, Better, Faster, Stronger: Large-scale QM and QM/MM for Predictive Modeling in Enzymes and Proteins, *Curr. Opin. Struct. Biol.*, 2022, **72**, 9–17.
15 M. Wang, P. Li, X. Jia, W. Liu, Y. Shao, W. Hu, J. Zheng, B. R. Brooks and Y. Mei, Efficient Strategy for the Calculation of Solvation Free Energies in Water and Chloroform at the Quantum Mechanical/Molecular Mechanical Level, *J. Chem. Inf. Model.*, 2017, **57**, 2476–2489.
16 J. Gao, Absolute Free Energy of Solvation from Monte Carlo Simulations Using Combined Quantum and Molecular Mechanical Potentials, *J. Phys. Chem.*, 1992, **96**, 537–540.
17 V. Luzhkov and A. Warshel, Microscopic Models for Quantum Mechanical Calculations of Chemical Processes

Open Access Article. Published on 13 May 2024. Downloaded on 8/2/2025 6:55:55 AM. This article is licensed under a Creative Commons Attribution-NonCommercial 3.0 Unported Licence.

in Solutions: LD/AMPAC and SCAAS/AMPAC Calculations of Solvation Energies, *J. Comput. Chem.*, 1992, **13**, 199–213.
18 M. A. Olsson and U. Ryde, Comparison of QM/MM Methods to Obtain Ligand-Binding Free Energies, *J. Chem. Theory Comput.*, 2017, **13**, 2245–2253.
19 P. Li, X. Jia, X. Pan, Y. Shao and Y. Mei, Accelerated Computation of Free Energy Profile at *ab Initio* Quantum Mechanical/Molecular Mechanics Accuracy *via* a Semi-Empirical Reference Potential. I. Weighted Thermodynamics Perturbation, *J. Chem. Theory Comput.*, 2018, **14**, 5583–5596.
20 W. Hu, P. Li, J.-N. Wang, Y. Xue, Y. Mo, J. Zheng, X. Pan, Y. Shao and Y. Mei, Accelerated Computation of Free Energy Profile at *Ab Initio* Quantum Mechanical/Molecular Mechanics Accuracy *via* a Semiempirical Reference Potential. 3. Gaussian Smoothing on Density-of-States, *J. Chem. Theory Comput.*, 2020, **16**, 6814–6822.
21 A. Rizzi, P. Carloni and M. Parrinello, Targeted Free Energy Perturbation Revisited: Accurate Free Energies from Mapped Reference Potentials, *J. Phys. Chem. Lett.*, 2021, **12**, 9449–9454.
22 X. Pan, P. Li, J. Ho, J. Pu, Y. Mei and Y. Shao, Accelerated Computation of Free Energy Profile at *Ab Initio* Quantum Mechanical/Molecular Mechanical Accuracy *via* a Semi-empirical Reference Potential. II. Recalibrating Semi-empirical Parameters with Force Matching, *Phys. Chem. Chem. Phys.*, 2019, **21**, 20595–20605.
23 J.-N. Wang, W. Liu, P. Li, Y. Mo, W. Hu, J. Zheng, X. Pan, Y. Shao and Y. Mei, Accelerated Computation of Free Energy Profile at *Ab Initio* Quantum Mechanical/Molecular Mechanics Accuracy *via* a Semiempirical Reference Potential. 4. Adaptive QM/MM, *J. Chem. Theory Comput.*, 2021, **17**, 1318–1325.
24 T. J. Giese and D. M. York, Development of a Robust Indirect Approach for MM → QM Free Energy Calculations That Combines Force-Matched Reference Potential and Bennett's Acceptance Ratio Methods, *J. Chem. Theory Comput.*, 2019, **15**, 5543–5562.
25 M. Wang, Y. Mei and U. Ryde, Host-Guest Relative Binding Affinities at Density-Functional Theory Level from Semiempirical Molecular Dynamics Simulations, *J. Chem. Theory Comput.*, 2019, **15**, 2659–2671.
26 R. W. Zwanzig, High-Temperature Equation of State by a Perturbation Method. I. Nonpolar Gases, *J. Chem. Phys.*, 1954, **22**, 1420–1426.
27 J. G. Kirkwood, Statistical Mechanics of Fluid Mixtures, *J. Chem. Phys.*, 1935, **3**, 300–313.
28 C. H. Bennett, Efficient Estimation of Free Energy Differences from Monte Carlo Data, *J. Chem. Phys.*, 1976, **22**, 245–268.
29 M. R. Shirts and J. D. Chodera, Statistically Optimal Analysis of Samples from Multiple Equilibrium States, *J. Chem. Phys.*, 2008, **129**, 124105.
30 C. Cave-Ayland, C.-K. Skylaris and J. W. Essex, Direct Validation of the Single Step Classical to Quantum Free Energy Perturbation, *J. Phys. Chem. B*, 2015, **119**, 1017–1025.
31 G. König, P. S. Hudson, S. Boresch and H. L. Woodcock, Multiscale Free Energy Simulations: An Efficient Method for Connecting Classical MD Simulations to QM or QM/MM Free Energies Using Non-Boltzmann Bennett Reweighting Schemes, *J. Chem. Theory Comput.*, 2014, **10**, 1406–1419.
32 J.-N. Wang, Y. Xue, P. Li, X. Pan, M. Wang, Y. Shao, Y. Mo and Y. Mei, Perspective: Reference-Potential Methods for the Study of Thermodynamic Properties in Chemical Processes: Theory, Applications, and Pitfalls, *J. Phys. Chem. Lett.*, 2023, **14**, 4866–4875.
33 U. Ryde, How Many Conformations Need to Be Sampled to Obtain Converged QM/MM Energies? The Curse of Exponential Averaging, *J. Chem. Theory Comput.*, 2017, **13**, 5745–5752.
34 S. Boresch and H. L. Woodcook, Convergence of Single-step Free Energy Perturbation, *Mol. Phys.*, 2017, **115**, 1200–1213.
35 P. V. Klimovich, M. R. Shirts and D. L. Mobley, Guidelines for the Analysis of Free Energy Calculations, *J. Comput.-Aided Mol. Des.*, 2015, **29**, 397–411.
36 J. Heimdal and U. Ryde, Convergence of QM/MM Free-energy Perturbations Based on Molecular-mechanics or Semiempirical Simulations, *Phys. Chem. Chem. Phys.*, 2012, **14**, 12592–12604.
37 J. Kästner, H. M. Senn, S. Thiel, N. Otte and W. Thiel, QM/MM Free-Energy Perturbation Compared to Thermodynamic Integration and Umbrella Sampling: Application to an Enzymatic Reaction, *J. Chem. Theory Comput.*, 2006, **2**, 452–461.
38 A. Pohorille, C. Jarzynski and C. Chipot, Good Practices in Free-Energy Calculations, *J. Phys. Chem. B*, 2010, **114**, 10235–10253.
39 C. Dellago and G. Hummer, Computing Equilibrium Free Energies Using Non-Equilibrium Molecular Dynamics, *Entropy*, 2014, **16**, 41–61.
40 T. H. Rod and U. Ryde, Accurate QM/MM Free Energy Calculations of Enzyme Reactions: Methylation by Catechol O-Methyltransferase, *J. Chem. Theory Comput.*, 2005, **1**, 1240–1251.
41 P. Mikulskis, S. Genheden and U. Ryde, A Large-Scale Test of Free-Energy Simulation Estimates of Protein–Ligand Binding Affinities, *J. Chem. Inf. Model.*, 2014, **54**, 2794–2806.
42 N. Lu and D. A. Kofke, Accuracy of Free-energy Perturbation Calculations in Molecular Simulation. I. Modeling, *J. Chem. Phys.*, 2001, **114**, 7303–7311.
43 D. Wu and D. A. Kofke, Phase-space Overlap Measures. I. Fail-safe Bias Detection in Free Energies Calculated by Molecular Simulation, *J. Chem. Phys.*, 2005, **123**, 054103.
44 D. Wu and D. A. Kofke, Model for Small-sample Bias of Free-energy Calculations Applied to Gaussian-distributed Nonequilibrium Work Measurements, *J. Chem. Phys.*, 2004, **121**, 8742–8747.
45 N. Lu and D. A. Kofke, Accuracy of Free-energy Perturbation Calculations in Molecular Simulation. II. Heuristics, *J. Chem. Phys.*, 2001, **115**, 6866–6875.

 © 2024 The Author(s). Published by the Royal Society of Chemistry

Open Access Article. Published on 13 May 2024. Downloaded on 8/2/2025 6:55:55 AM.
This article is licensed under a Creative Commons Attribution-NonCommercial 3.0 Unported Licence.

46 D. Wu and D. A. Kofke, Phase-space Overlap Measures. II. Design and Implementation of Staging Methods for Free-energy Calculations, *J. Chem. Phys.*, 2005, **123**, 084109.
47 D. A. Kofke, On the Sampling Requirements for Exponential-work Free-energy Calculations, *Mol. Phys.*, 2006, **104**, 3701–3708.
48 D. M. Zuckerman and T. B. Woolf, Systematic Finite-Sampling Inaccuracy in Free Energy Differences and Other Nonlinear Quantities, *J. Stat. Phys.*, 2004, **114**, 1303–1323.
49 G. Hummer and A. Szabo, Calculation of Free-energy Differences from Computer Simulations of Initial and Final States, *J. Chem. Phys.*, 1996, **105**, 2004–2010.
50 G. Hummer, Fast-growth Thermodynamic Integration: Error and Efficiency Analysis, *J. Chem. Phys.*, 2001, **114**, 7330–7337.
51 V. Ekberg and U. Ryde, On the Use of Interaction Entropy and Related Methods to Estimate Binding Entropies, *J. Chem. Theory Comput.*, 2021, **17**, 5379–5391.
52 C. Jarzynski, Nonequilibrium Equality for Free Energy Differences, *Phys. Rev. Lett.*, 1997, **78**, 2690–2693.
53 P. S. Hudson, H. L. Woodcock and S. Boresch, Use of Nonequilibrium Work Methods to Compute Free Energy Differences between Molecular Mechanical and Quantum Mechanical Representations of Molecular Systems, *J. Phys. Chem. Lett.*, 2015, **6**, 4850–4856.